Soft Matter

Accepted Manuscript

ROYAL SOCIETY OF CHEMISTRY

www.rsc.org/softmatter

ARTICLE TYPE www. rsc.org/xxxxxx | XXXXXXXX

Flows of living polymer fluids

Marc-Antoine Fardin[a,c] **and Sandra Lerouge**[*b,c‡]

Received Xth XXXXXXXXXX 20XX, Accepted Xth XXXXXXXXX 20XX
First published on the web Xth XXXXXXXXXX 200X
DOI: 10.1039/b000000x

We report on recent progress made on the flows of living polymer fluids. Such fluids have been model systems for rheological research for more than twenty years and they continue to be fascinating. Like most if not all soft matter systems, living polymers under flow show a strong feedback between the structure of the fluid and that of the flow, the first influencing the second and vice-versa. In our opinion, such interplay between microscopic kinetics and macroscopic kinematics has historically been mostly understood from a "structural perspective", in the tradition of physical chemistry. Nevertheless, in recent years a more "hydrodynamical perspective" has emerged by making fruitful analogies with elastic and inertio-elastic instabilities known in solutions of regular polymers. We also underline how this new perspective constrains theoretical modelling and calls for the use of new tools of investigation.

1 Introduction

From the rich variety of self-assembled architectures at the microscopic scale to hydrodynamic instabilities at the macroscopic scale, surfactant solutions continue to fascinate us. Fig. 1 gives a schematic description of various time and length scales of interest[1]. At the atomic scale, one can ask about the different chemical routes leading to amphiphilic surfactant molecules[2]. One can then ask about the self-assembly of multiple surfactants molecules into micelles of various architectures. Depending on the packing properties of the surfactants, cylindrical micelles can form and grow in length as the surfactant concentration increases, forming objects similar to polymers, but with the ability to constantly break and fuse. Here, we will focus on flows of these so-called "living polymers". The scale of the polymeric Kuhn segments (persistence length) shall be our most microscopic scale.

In recent years, living polymers have mostly been called by the umbrella term "wormlike micelles", but recalling the similarity with polymer solutions can help make fruitful analogies. The most important difference with regular (non-living) polymers is that length and concentration of wormlike chains are not independent parameters. At low concentration, micelles are little, isolated rods. As the concentration increases, so does the length of the micelles, which go from being rod-like to being closer to the shape of common earthworms, with multiple Kuhn segments along their length. Like polymers,

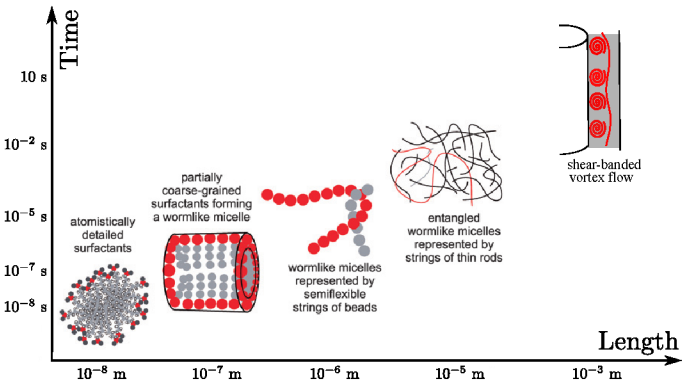

Fig. 1 Time and length scales involved in micellar solutions, from the molecular scale to the hydrodynamic scale. The shortest length and time scales are associated with the surfactant molecules. Increasing the surfactant concentration leads to the formation of micellar aggregates which can keep increasing in length to form highly flexible cylinders. The growth of the micellar aggregates can be easily promoted by addition of mineral salts or strongly binding counterions. At sufficiently high surfactant concentration the resulting wormlike micelles form a viscoelastic entangled network. Finally, the largest length and time scales involved in the flow correspond to the characteristic size and time of the flow itself and are typically associated with the development of hydrodynamical flow patterns. Adapted from Padding *et al.*[1], by permission of The Royal Society of Chemistry.

[a] *Université de Lyon, Laboratoire de Physique, École Normale Supérieure de Lyon, CNRS UMR 5672, 46 Allée d'Italie, 69364 Lyon Cédex 07, France.*
[b] *Laboratoire Matière et Systèmes Complexes, CNRS UMR 7057, Université Paris-Diderot, 10 rue Alice Domon et Léonie Duquet, 75205 Paris Cédex 13, France. E-mail: sandra.lerouge@univ-paris-diderot.fr*
[c] *The Academy of Bradylogists*

those worms can entangle, and at even higher concentration, their semi-flexibility can give rise to nematic phases[3]. Under macroscopic flow, dilute, entangled, and ordered phases of living polymers give rise to different rheological signatures such as shear-thickening, shear-thinning (which can be extreme, i.e. shear-banding), or combinations of the two[4]. These nonlinear rheological behaviors are associated with strong modifications both of the internal structure of the fluid and of the flow field, i.e. of the microscopic and macroscopic properties. In practice, the two poles–micro and macro–are usually studied by different groups, in different labs, partly due to material constraints but mostly for historical reasons. The experimental devices required to study the microscopic structure of micellar fluids are not the same as those used to observe flow instabilities. Historically, the effect of an external flow field on the microstructure of wormlike micelles was investigated essentially from the point of view of physical chemistry. For some time each vantage point essentially ignored the other. Nevertheless, in the last five years some studies have started to call for a framework that could be applicable to the description of phenomena happening on multiple scales. How are macroscopic flows and their kinematics impacted by the kinetics of the microscopic structure of the fluid, and vice versa? How does the structure of the fluid depend on the structure of the flow? When moving from the microscopic to the macroscopic, what is coarse-grained out of the picture, and what becomes relevant? When moving the other way around, should we worry about ways in which flow instabilities could alter measurements of microscopic properties? These are the types of questions that emerge when the two vantage points start to face each other.

In the first section we shall highlight recent studies pertaining to what we will call the "structural approach", i.e. the more microscopic vantage point. In the second section we shall highlight studies pertaining to the dual approach, which we will call "hydrodynamical", i.e. the more macroscopic vantage point. To tackle the challenges raised by facing the two perspectives, we will discuss the recent insight offered by new theoretical models and new tools of investigation, which will be discussed in the last two sections. Note that this highlight article mostly focuses on the recent literature. For more details of the older literature, the reader can refer to different experimental and theoretical reviews[3–9].

2 Structural approach

Living polymers, like any complex fluids, have a microscopic structure that can be altered by common flows. The flow can modify the structure, which can in turn modify the flow. This is one of the two directions in which the feedback loop between flow and structure can be read. Dilute solutions of rod-like micelles give a perfect example of such phenomenology.

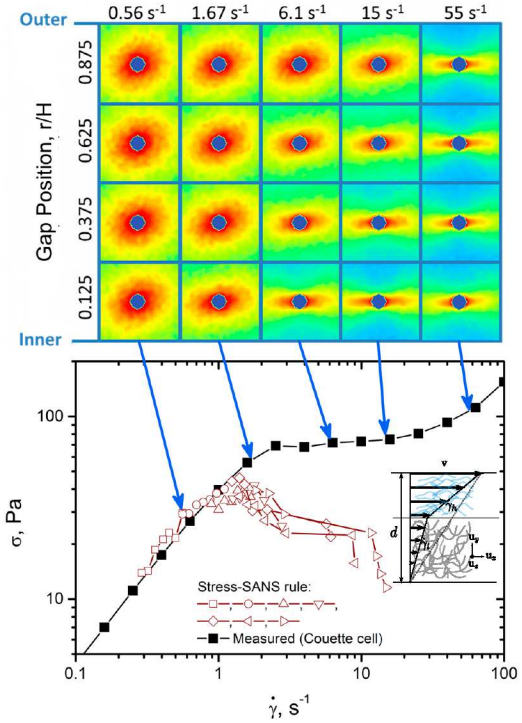

Fig. 2 Top: SANS patterns at representative gap positions and nominal shear rates as indicated. The experiments are performed on the system CPCl/NaSal/D_2O in 0.5 M NaCl ($\phi = 6.6\%$). SANS patterns are measured in a Taylor-Couette (TC) cell with an inner radius $R_i = 25$ mm, a gap width $d = 1$ mm and a height $h = 5$ mm, while the rheological data are collected in a standard TC cell. The typical acquisition time of the SANS spectra is about 15 min. Bottom: Measured shear stress versus nominal shear rate and the calculated shear stresses from analysis of the SANS patterns, velocimetry measurements, and the stress-SANS rule. The inset shows a scheme of the banding structure associated with the stress plateau. Adapted from Gurnon *et al.* [13] with permission from the American Chemical Society.

In the zero-shear limit, the viscosity of dilute solutions is close to that of water, simply slightly renormalized by the presence of the colloids. But as shear rate builds up, a structure that is more viscous than the suspending solvent is induced, generating a large increase of the apparent viscosity; we speak of shear-induced structures (SIS). The SIS are associated with a transition from rod-like to wormlike micelles and exhibit a viscoelastic character[4]. As concerns such shear-thickening transitions, in our opinion, no significant new insights about the properties of the SIS and the underlying mechanism of shear-induced growth have been published in the recent years[10–12].

More progress has been made concerning the flow of entangled solutions. In particular, special attention has been paid to shear-banding systems, either semi-dilute or concentrated. The shear-banding transition is characterized by the segrega-

tion of the flow field into at least two macroscopic layers of differing local shear rates, $\dot{\gamma}_l$ and $\dot{\gamma}_h$, stacked along the velocity gradient direction and coexisting at constant stress (Fig. 2 bottom - inset). The shear bands have different viscosities and consequently different internal microstructures. In addition to the classical techniques of investigation of the microstructure that had already been used in the past, such as flow birefringence [14], small angle neutron (SANS) [15] or light scattering [16], and nuclear magnetic resonance (NMR) spectroscopy [17,18], other techniques have been implemented recently, such as diffusing wave spectroscopy [19] or conductivity [20,21]. Since 2004, most of these experimental techniques have been improved to give a space- and time-resolved description of the flow/structure feedback in wormlike micelles (for reviews on the subject see Refs [4,7,8]). However the most recent developments arose from the combination of global rheology, 1D velocimetry and spatially-resolved small angle neutron scattering [13,22–26]. The additional capability provided by the latter technique is pointwise measurements of the neutron scattering intensity in the flow-flow gradient plane of a Taylor-Couette (TC) cell. The results collected recently in this framework unambiguously confirmed previous interpretations: shear-banding in concentrated samples is related to a shear-induced isotropic to nematic transition [22,23,25] while, in semi-dilute samples, it corresponds to a coexistence of flow-aligned wormlike micelles of low viscosity in the high shear rate band with entangled wormlike micelles of higher viscosity in the low shear rate band [13] (Fig. 2 Top). SANS measurements present a direct analogy with flow birefringence measurements since they provide insights into the segmental alignment of wormlike micelles (orientation and degree of anisotropy). Exploiting this analogy, a stress-SANS rule similar to the well-known stress-optical rule was derived [23], providing a direct comparison with global rheological data with the serious limitation that both are restricted to a correct description of the linear regime but fail once non-linearities dominate. More interestingly, from this elegant pointwise SANS technique, spatial profiles of volume fraction of surfactant were determined using absolute neutron transmission measurements. For concentrated samples, macroscopic concentration gradients were observed, consistent with the development of a concentrated paranematic phase at the expense of the isotropic phase [25] while no significant concentration differences were detectable for semi-dilute samples [13]. These results constitute a first step towards a better understanding of the role of flow-concentration coupling in shear-induced phase separation, and provide a way to test theoretical predictions [6,27]. Any further progress in this direction may lead to a more accurate description of the feedback loop between the flow and the microstructure. In this context, recent results describing the structure of the flow and gathered in all concentration ranges (see Section 3) showed that improvements of structural probes are still needed to overcome some limitations inherent to these techniques. In particular, long-time recording is required to get reasonable statistics to collect representative scattering patterns so that the structural picture is time-averaged, limiting the exploration of unsteady flows. The combination with 1D velocimetry is valuable and clearly goes in the right direction but is not sufficient for making conclusions regarding the existence of stable steady-state shear-banding [28]. Furthermore, even when they are spatially resolved along the velocity gradient direction, imaging techniques at the microscopic scale such as flow birefringence and SANS always give information averaged over the neutral or vorticity direction. We will see in the following that the interpretation of such data could be misled by the presence of flow instability. In particular, the shape of the orientation profiles strongly depends on the structure of the flow [13,29,30] (see Fig. 3a-i) and has to be interpreted with great care.

3 Hydrodynamical approach

The structural approach tends to assume a fixed macroscopic flow and investigates its impact on the microstructure. In contrast, the hydrodynamical approach tends to assume a fixed microstructure of the fluid and investigates its impact on the flow. As suggested by etymology, the hydro-dynamical approach is readily applicable in Newtonian fluids like water. The only non-vanishing material function is viscosity, which–still–depends on the kinetics of the constituents. Then, given a value of viscosity, one can ask what would be the thresholds in shear rate above which a flow becomes unstable and eventually turbulent. The focus here is not on the kinetics at the microscopic scale, but on the kinematics at the macroscopic scale. Until recently, the notion of hydrodynamic flow instability was systematically associated with inertia, and so to the value of the Reynolds number $Re = \tau_i \dot{\gamma}$, where $\dot{\gamma} \sim U/d$ is the characteristic shear rate and $\tau_i \equiv d^2/\nu$ is the viscous diffusion time (U is the characteristic velocity, d the width in the velocity gradient direction, and ν the kinematic viscosity). Nevertheless, since 1990 it is known that flow instabilities can occur in complex fluids with vanishing inertia [38]. For instance, combining experiments on polymer solutions and linear stability analysis of viscoelastic models, Larson *et al.* showed that a purely elastic instability mechanism exists in Taylor-Couette flow [39]. In the small gap limit, one only needs to replace the Reynolds number by the Weissenberg number in the definition of the relevant Taylor number, i.e. $Ta \equiv \Lambda^{1/2} Wi$, with $Wi \equiv \tau_e \dot{\gamma}$, where τ_e is the viscoelastic relaxation time, and $\Lambda \equiv d/R_i$ is the dimensionless curvature of the streamlines (R_i is the inner radius of the TC device). Note that in some cases, in particular for wormlike micelles, the ratio between the first normal stress difference and the shear stress can provide a good estimate of Wi. For $Ta > m$, counter-rotating Taylor-like vortices emerge

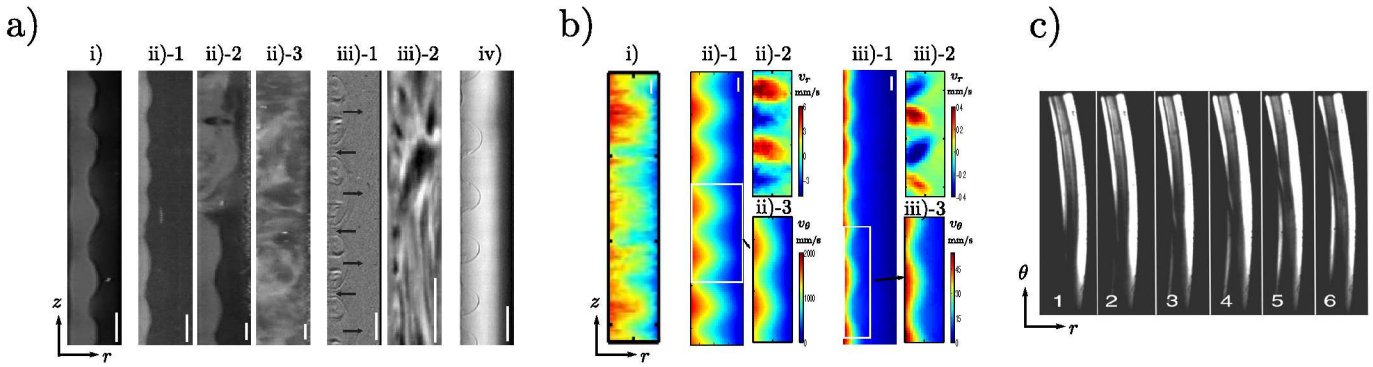

Fig. 3 Evidence for elastic instability and turbulence in the Taylor-Couette flow of wormlike micelles. (a) View of the gap of the TC cell in the (r,z) flow gradient-vorticity plane for various shear banding systems belonging to the semi-dilute and concentrated regimes. Depending on the native turbidity of the high shear rate band, the gap of the TC cell is illuminated with either laser light or white light, the latter providing direct visualisation of the vortex structure responsible for the undulation of the interface. The gap size (1.13 mm) corresponds to the width of the picture while the bar (1 mm) gives the vertical scale. The height and the inner radius of the TC cell are respectively 40 mm and 13.33 mm. (i) CPCl/NaSal/$H_2$0 in 0.5 M NaCl ($\phi = 6.3$ %, $T = 21.5$°C, $\dot{\gamma} = 9$ s^{-1}). (ii) CPCl/NaSal/H_2O in 0.5 M NaCl ($\phi = 10$ %, $T = 21.5$°C), (ii)-1 $\dot{\gamma} = 8$ s^{-1}, (ii)-2 $\dot{\gamma} = 15$ s^{-1}, (ii)-3 $\dot{\gamma} = 20$ s^{-1}, (iii) CTAB(0.3 M)/$NaNO_3$ (0.405 M) ($\phi = 11$ %, $T = 28$°), (iii)-1 $\dot{\gamma} = 40$ s^{-1}, (iii)-2 $\dot{\gamma} = 140$ s^{-1}, (iv) CTAB/D_2O ($\phi = 20$ %, $T = 37.5$°C, $\dot{\gamma} = 50$ s^{-1}). Reproduced from Refs [28,30–33]. b) Velocity map deduced from ultrasonic imaging for various (shear-thickening, non-shear banding and shear banding) systems. The gap size (2 mm) corresponds to the width of the picture while the bar (2 mm) gives the vertical scale. The height and the inner radius of the TC cell are 60 mm and 23 mm respectively. (i) (ii)-1 and (iii)-1 : $v_\theta(r,z)$ respectively for CTAT ($\phi = 0.16$ %, $T = 25$°C, $\dot{\gamma} = 50$ s^{-1}), CTAB(0.1 M)/$NaNO_3$(0.3 M) ($\phi = 4$ %, $T = 30$°C, $\dot{\gamma} = 1000$ s^{-1}) and CTAB(0.3 M)/$NaNO_3$(0.405 M) ($\phi = 11$ %, $T = 30$°C, $\dot{\gamma} = 40$ s^{-1}). (ii)-2 and (ii)-3 enlargements showing respectively the radial (v_r) and azimuthal (v_θ) velocity maps. Reprinted from Refs [34–36]. (c) View of the gap of the Taylor-Couette cell ($d = 0.5$ mm and $R_i = 28.5$ mm) between crossed polarisers in the (θ,r) flow - flow gradient plane for a shear banding system made of CTAB (0.05 M)/NaSal (0.1 M) ($\phi \simeq 2.5$ %, $\dot{\gamma} = 5$ s^{-1}, $T = 23$°C). Reprinted from Decruppe *et al.* [37]. All figures are reproduced by permission of The Royal Society of Chemistry, the American Physical Society or The European Physical Journal.

(e.g. with $m \simeq 6$ for the Upper-Convected Maxwell model[39]).

In a Newtonian fluid, the rule of thumb is that if Re becomes large, flow instabilities are to be expected. In a viscoelastic non-Newtonian fluid, considering that flow instabilities will emerge if Wi becomes large also seems to be a useful guideline[40]. When both Re and Wi are large, the situation is more complicated, but dimensional arguments suggest that the relevant Taylor number for so-called "inertio-elastic instabilities" should be of the form $Ta = \Lambda^{1/2} S$, with $S = f(Re, Wi)$, such that $\lim_{\mathscr{E}\to 0} S = Re$ and $\lim_{\mathscr{E}\to\infty} S = Wi$, where $\mathscr{E} \equiv Wi/Re$[41,42].

Recently, the validity of this phenomenology, originally developed around polymer solutions, was successfully extended to flows of surfactant solutions[36,43]. Here again, the dilute regime can be used as an example. In a study published this year, it was shown that the well-known shear-thickening transition can be accompanied by flow instabilities[34]. Before the formation of SIS, the fluid is almost identical to pure water in terms of apparent viscosity, with $\mathscr{E} \sim 0$ and instabilities are driven by inertia, i.e. controlled by Re. After the formation of SIS, the viscosity rises and normal stresses build up to a point where $\mathscr{E} \gtrsim 1$. In this shear-thickening regime, the instabilities are dominated by elasticity, i.e. controlled by Wi[34] (e.g. Fig. 3b-i). These recent results call for a re-interpretation of most of the data gathered on shear-thickening dilute systems, where fluctuating behaviors and so-called "vorticity-banding"[44,45] are most likely connected to vortex flows[46–50]. Recent studies on turbulent drag reduction by surfactant additives could also benefit from a more systematic estimation of Re and Wi, and the potential interplay of inertial and elastic instabilities[51–56].

The viscoelastic instability phenomenology was invoked earlier to explain the fluctuating behaviors that had been observed in an ubiquitous way in shear-banding flows of entangled solutions (semi-dilute and concentrated)[43]. At first, the secondary vortex flow on top of the shear-banded base flow was only evidenced through the oscillations of the interface between the bands that it generated in the vorticity/velocity-gradient plane[30] (e.g. Fig. 3a-i). It was then imaged more directly using techniques from white light imaging (e.g. Fig. 3a-iii-1) and traditional anisotropic tracers[31], to recently developed 2D ultrasonic velocimetry[36,57] (e.g. Fig. 3b). The appropriate TC scaling of the viscoelastic instability for shear-banded flows was worked out in 2011[58], giving rise to the prediction of three types of shear-banding flows depending on their stability. The existence of the three types of flows

was subsequently confirmed by experiments on a large set of conditions, with various types and concentrations of surfactant and salt, varying temperatures, and various TC geometries[33]. The essential conclusion is that the instability is due to the high first normal stress difference (i.e. high local Weissenberg number $Wi_h = \tau_e \dot{\gamma}_h$) in the induced band, which acts as an effective gap with dimensionless curvature $\Lambda_\alpha = \alpha d/R_i$, where $\alpha(\dot{\gamma}) \in [0,1]$ is the proportion of induced (high shear rate) band[42,58]. As the shear rate is increased, a variety of more or less complex spatio-temporal patterns is observed[33].

Note that when the vortex flow generated by viscoelastic instability is coherent, there is no particular signature of the instability in the 1D velocity profiles (i.e. no noticeable level of fluctuations in the local azimuthal velocity)[59]. The existence or absence of secondary flows can only be attested reliably by 2D measurements. On the other hand, the largest and most obvious fluctuating behaviors have been associated with turbulent bursts (e.g. Fig. 3a-ii) and other manifestations of elastic turbulence[32,59,60] (e.g. Fig. 3a-iii-2). These results prompted a new reading[61] of the phenomenon initially considered as "rheochaos"[62–64].

When instabilities develop on shear-banded base flows of wormlike micelles, the resulting secondary flows have noticeable differences with the flow patterns observed in homogeneous solutions of polymers. We will see in section 4 that this may be due to the interaction between the usual bulk modes of instability and modes associated with the interface between the bands. In order to underline the similarities rather than the differences between living and regular polymers, a study recently investigated the instability of a homogeneous–non shear-banding–solution of wormlike micelles. The conditions investigated corresponded to an elasticity $\mathscr{E} \sim 1$, and the flow patterns were very similar to those observed at similar values of $\mathscr{E}$ in polymer solutions[35]. The ultrasonic velocimetry technique that was used also allowed the measurement of the radial velocity field, which revealed an asymmetry unseen in inertial vortex flows (e.g. Fig. 3b-ii-2 and b-iii-2).

Most recent progress in the hydrodynamical approach came from experiments performed in TC geometries mounted on standard rheometers but modified to allow for flow visualisation of some type. Nevertheless, it is important to underline that the TC case is a prototype for the Taylor-Görtler mechanism occurring in any other curved flow dominated by shear[42]. When the base flow has mixed kinematics, like in entry flow[65], or flows behind cylinders[66,67] or spheres[68], the interpretation is subtler, but the viscoelastic instability phenomenology should remain applicable. We shall discuss flows dominated by extension in section 5.

4 Theory

Since the 80s shear-banding has been the subject of many theoretical studies[5]. Shear-banding is ubiquitous in entangled micellar solutions so most theoretical studies focus on them; studies on dilute or ordered phases are much more scarce, and to the best of our knowledge, none came out in the last five years. Again, two approaches must be distinguished: one rather microscopic and the other rather macroscopic.

The first approach could be called reductionist or bottom-up; in other words it starts from a structural perspective, gets validated by a comparison with microscopic data, and tries to compute predictions of macroscopic phenomena. Cates' reptation-reaction model remains the prime example for such an approach[5]. In the early 90s, Cates *et al.* modified the reptation model of polymers in order to include the constant breaking and recombination of micelles. The model not only predicted the correct distribution of micellar lengths, but also the associated linear rheology and even the onset of shear-banding. Nevertheless, the model was hardly tractable when used to predict realistic macroscopic flows. It is also important to note that shear-banding in Cates' model was not associated with the living property of the polymers. On the contrary, shear-banding was already a feature of the Doi-Edwards (DE) model used to model regular polymers[5]. Because no shear-banding seemed to be observed in polymer solutions, the DE model was extended to include the so-called "convective constraint release" (CCR) mechanism[69]. Depending on the degree of CCR, shear-banding could be removed. Some arguments were then made to explain the difference in degree of CCR between micellar solutions and polymer solutions[70]. These arguments and other modern additions to the DE model were recently included in Cates' model[71]. Note that determining if shear-banding can be at play in polymer solutions remains a topic of active debate. This controversy may find its roots in the conclusion of a recent broader theoretical study which concerns the connection between steady shear-banding flows observed in entangled solutions of living polymers and other transient shear-banding flows observed in polymeric and soft glassy materials[72].

The second approach could be called phenomenological or top-down; in other words it starts from an hydrodynamic perspective, gets validated by a comparison with macroscopic data, and may try to connect its parameters to microscopically relevant quantities. The diffusive Johnson-Segalman (dJS) model originally developed by Olmsted *et al.* remains the prime example for such an approach. In recent years, a version of the dJS model with diffusion on velocity gradient rather than stress was used to obtained an analytical solution of the shear-banded flow in simple shear[73,74]. This solution was used to highlight the systematic interplay between wall slip and shear-banding flows[74], which had been underlined in

recent experiments[8,28,59,75–78] and in simulations[79]. Stability analysis of the dJS model was also performed in order to confirm the preponderance of bulk modes of viscoelastic instability of the high shear rate band in TC flows[80,81]. Since the bulk modes depend on the curvature of the streamlines (Λ_α), they vanish at the onset of shear-banding, where $\alpha \to 0$. Within this limit, interfacial modes related to the jumps in normal stress differences between the bands are likely to become preponderant[81]. The agreement between dJS predictions and experiments is good, but some discrepancies remain. In particular, the linear stability analysis predicts that the first instability should be non-axisymmetric[81], whereas most secondary flows in experiments appear to be axisymmetric[43]. Nevertheless, one recent experiment did show the presence of some oscillating behavior in the flow direction[37] (see Fig. 3c). Overall, the dJS model has remained a useful guide on the macroscopic behaviors of shear-banding wormlike micelles. The major shortfall of the model comes from the absence of a relationship between its parameters and microscopic dynamics. Most importantly, the so-called "slip parameter" a of the dJS model (which needs to be different from ± 1 to produce shear-banding) does not have a rigorous connection to the kinetics of the fluid structure.

The difficulty in reconciling microscopic and macroscopic models is not at all unique to living polymers; it is an outstanding problem in soft matter research in general[82]. To bridge the gap between the two perspectives, one usually invokes some type of mesoscopic kinetic theory. For instance, it is well-known that the Oldroyd B model of viscoelasticity can be obtained by summing up the dynamics of mesoscopic elastic dumbbells in a viscous solvent. Such cross-over theory allows a connection between the macroscopic relaxation time and the ratio of the drag on the dumbbells and their elasticity $\tau_e \equiv \mu/K_0$. The drag coefficient μ and elasticity K_0 can then be connected to more fine-grained dynamics. Such a relation does not exist for the dJS parameter a. In contrast, the diffusive Giesekus model has a parameter similar to a but with a clearer connection to anisotropic drag at a mesoscopic level[83]. For that reason, the diffusive Giesekus model has been preferred over the dJS model in some recent studies[22,23,25], since the macroscopic predictions are otherwise similar.

Other recent progress on the theory of wormlike micelles is similarly placed at the cross-over between microscopic and macroscopic modelling. For instance, some progress has been made on the Bautista-Manero-Puig model (BMP), which is built on extended thermodynamics[84–89]. Nevertheless, some issues of this model related to the selection of the stress plateau in the shear-banding regime remain[74]. Another route has been taken with the Vasquez-Cook-McKinley (VCM) model[90–93]. This model proposes to coarse-grain the broad distribution of micellar lengths in an entangled solution to a set of two species, one short and one twice as long. The breaking/recombination kinetics are then taken into account by allowing the short species to fuse into larger pieces, which can in turn break. The VCM model can predict shear-banding at least as well as the dJS model and can also be used to perform stability analysis of shear-banded flows[94]. Originally, the VCM model was thought of as a simplification of Cates' model[95]. Nevertheless, it is important to point out that shear-banding has a different origin in the two models. In Cates' model, shear-banding is a consequence of the shear-induced tube alignment of the DE model, which cannot be tamed due to a weak level of CCR. In contrast, shear-banding in the VCM model is a consequence of shear-induced breakage of long species into short ones, as recently reported from a nonequilibrium thermodynamical approach[93].

5 New tools of investigation

Many recent studies going beyond what we reviewed so far have used microfluidic tools of investigation, i.e. flow geometries with a sub-millimeter scale d. From an hydrodynamic perspective, microfluidics allows reaching very high shear rates (because $\dot{\gamma} \sim d^{-1}$) while remaining inertialess (because $\tau_i \sim d^2$). The first studies on living polymers indeed used microfluidics to obtain high shear rheology data in straight channel flows[99,100]. In straight channels, the curvature of the streamlines vanishes and the Taylor-Görtler mechanism of instability (see section 3) is ineffective. Nevertheless, in shear-banded flows, the stratification of normal stresses can lead to interfacial instability mechanisms generating streamwise vortices and unsteady flows, as shown both experimentally[96] and theoretically[94,96,101,102] (see Fig. 4a). A nonlinear transition to elastic turbulence is also a theoretical possibility[40].

Microfluidic channel flows were also used as a mean to probe so-called "non-local effects" in shear-banding wormlike micelles[103,104]. Such non-local effects are evidenced by a difference between the global flow curve measured on macroscopic rheometers and that obtained by using the relationship between the local stress and the measured shear rate in microchannels. The term "non-local" is somewhat misleading. It comes from the fact that differences between global and local rheologies are a consequence of the diffusive terms associated to shear-banding models (d-JS, *diffusive*-Giesekus, and VCM). Such diffusive terms usually apply to stresses or shear rate. In shear-banding wormlike micelles, the length $\ell = \sqrt{\mathscr{D}\tau_e}$ associated with the diffusivity $\mathscr{D}$ typically gives the width of the interface between the bands. The most recent measurements suggest that this length is between 1 and 10 μm[43,103,104]. In general, non-local effects should be expected when $\xi \equiv \ell/d \gtrsim 0.1$[74]. Many open questions remain regarding non-local effects. Are non-local effects related to wall slip[74]? What is the microscopic origin of $\mathscr{D}$? What is the interaction between non-local effects and flow instabilities? In

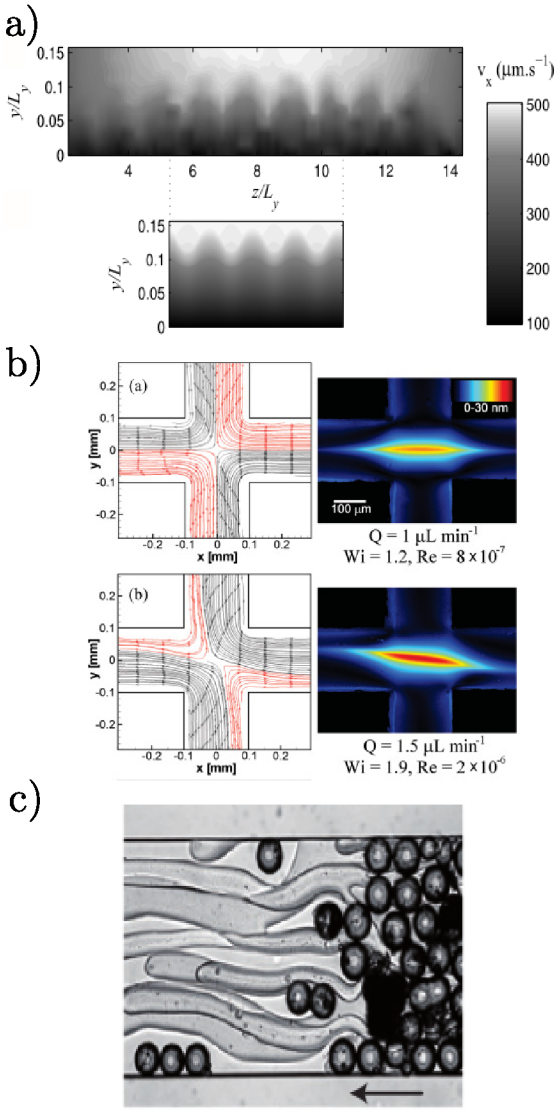

Fig. 4 a) Top : Greyscale of the experimentally measured velocity component v_x for a given pressure drop in a straight microchannel of rectangular cross-section (L_x =5 cm, L_y =64 μm, L_z =1 mm). The shear-banding micellar system is CTAB (0.3 M)/$NaNO_3$ (0.405 M) at T = 26°C. The applied pressure gradient is $\partial_x P/G_b$=1.3 where $G_b = 3.10^2$ Pa.m^{-1} characterises the onset of shear banding. Bottom : Corresponding numerical snapshot of the fully developed pattern computed from the dJS model. Reproduced from Nghe *et al.*[96] with permission from the American Physical Society. b) Experimentally determined streamlines and retardation showing the development of asymmetric flow in the cross-slot geometry for a shear banding 100:60:0 mM CPyCl:NaSal:NaCl solution (T = 22°C) as the flow rate is increased: (top) steady symmetric flow, (bottom) bifurcated flow. Reprinted from Haward *et al.*[97] with permission from the American Physical Society. c) Gel formation from a surfactant solution CTAB (0.003 M)/ NaSal (0.003 M) flowing at a flow rate of 1.5 ml/h in a 500 μm channel packed with 50-100 μm particles to create a microporous medium flow. In contrast with pure shear flow, the resulting flow-induced structure has an irreversible character. Reprinted from Vasudevan *et al.*[98]

particular, in Nghe's study, which was focused on instabilities, non-local effects were not reported[96] where they should be expected, and in Masselon's studies, which were focused on non-local effects, instabilities were not reported[103,104] where they should be expected. A similarly awkward situation exists in theoretical studies[80,96], where in order to maintain the interfacial instability mechanism the values of $\mathscr{D}$ used are orders of magnitude smaller than what is measured experimentally[43].

Microfluidics was also used in recent years to study flows dominated by extension rather than shear. Extensional rheology is comparatively less understood than shear rheology in many complex fluids. A few studies used macroscopic devices to investigate the effect of extension on living polymers[105–110]. Nevertheless, such conditions usually lead to free surface flows, which further complicate the problem. In the last few years, a few studies on the cross-slot geometry gathered data of relevance to both macroscopic and microscopic perspectives. From a structural perspective, the microfluidic cross-slot geometry can be used to study the consequences of the coil-stretch transitions triggered near the stagnation point. In standard polymers, the coil-stretch transition has been observed directly at the scale of the polymer by using fluorescently labelled molecules[111]. For micelles, direct data on the coil-stretch transition are still very limited[112], but several recent studies have analysed the fine structure of the birefringence strand associated with the structural transition. Birefringence microscopy was used to investigate the difference in birefringence in channels flows of shear-thinning and shear-banding solutions of entangled micelles[113]. The technique was then used in conjunction with particle image velocimetry in cross-slot geometry, as shown in Fig. 4b, and in a contraction geometry[114]. In cross-slot, some structural differences were seen between shear-banding[97,115] and non shear-banding solutions[97,116]. Nevertheless, in both cases flow instabilities eventually disrupted the birefringence strand, as shown in Fig. 4b. The instability had been noticed first by Pathak and Hudson[117]. The same year, Arratia *et al.*[118] identified a similar flow bifurcation instability in an homogeneous solution of regular polymer, which was subsequently understood to be a consequence of viscoelasticity, but different from the Taylor-Görtler mechanism[119]. Haward *et al.* were the first to connect the instability seen in living and regular polymers[115], and to systematically study the impact of *Re*, *Wi*, and the shear-thinning index on the instability.

In a very recent study, Haward *et al.*[120] came back to the channel flow of the non shear-banding solution investigated by Ober *et al.*[113]. It was realized that the laminar flow observed at one altitude along the neutral direction of the channel by Ober was actually a smooth subpart of a flow that was globally unstable. The instability reported seems to be linked with the spatio-temporally intermittent nucleation of gel-like SIS. Indeed, the solution used sat at the boundary between the di-

lute and semi-dilute regime, where non-standard behaviors are known to occur[4], with the superposition of shear-thickening due to SIS on top of a shear-thinning curve[49]. The macroscopic flow curve of the fluid used by Ober and Haward did not show any signature of SIS, but confinement may well be a catalytic factor in the kinetics of SIS. Generally, the kinetics of SIS remain very elusive. Recent microfluidic studies managed to produce permanent flow-induced structures using confined flows with very high deformation and extensional rates [98,121–126], as shown in Fig. 4c. Such data are very valuable but their theoretical interpretation remains superficial, especially because no link has been established so far between permanent flow-induced structures and reversible SIS associated with the various nonlinear rheological behavior of wormlike micelles.

The nature of the cross-slot instability has yet to be elucidated, in regular polymers as much as in living polymers. Curvature of the streamlines does not seem to be a dominant factor, and extension rather than shear seems to be the dimensional control parameter. Nevertheless, the instability may also depend indirectly on the transient nature of any flow with a stagnation point. The extension of single chains undergoing coil-stretch transitions is typically parametrized by Wi, but given as a function of the strain $\gamma = \dot{\gamma}t$, where t is the residence time in the vicinity of the stagnation point[111,112]. The importance of this time scale for the microscopic coil-stretch transition may have some macroscopic impact on the flow asymmetry instability.

Generally, the study of unsteady flows of complex fluids remains in its infancy, and living polymers offer a great opportunity to investigate that research avenue. The recent growing interest in large amplitude oscillatory shear (LAOS) experiments[127] is likely to give a rich set of data on which to build further research. A recent paper investigated the main flow field during LAOS of living polymers in cone-and-plate geometry[128], another used SANS to gain information on the microstructure[129,130], and a couple of papers investigated theoretical aspects[131,132]. In an upcoming paper, we shall also discuss the onset of flow instability in LAOS[133].

6 Conclusions and perspectives

Living polymers–like many if not all soft matter systems–are characterized by a complex feedback between the structure of the fluid and its flow, between the microscopic and the macroscopic. This nonlinearity means that the attribution of a cause for a given effect is always somewhat problematic. A strictly bottom-up/structural/fluid-oriented approach is too restrictive, and so is a strictly top-down/hydrodynamical/flow-oriented approach.

On the structural side of the problem, part of recent activities has been focused on permanent flow-induced structures using confined flows with very high deformation and extensional rates of dilute and to a lesser extent semi-dilute solutions[98,121–126]. Nevertheless, the link has not yet been established between such permanent flow-induced structures and reversible SIS associated with the various nonlinear rheological behavior of wormlike micelles. The kinetics of formation of permanent or transient structures remain unknown. Understanding how structures form under the influence of other fields could be helpful, for instance in ultrasound-induced structures[134]. In the entangled regime, improved small angle neutron scattering techniques have recently been used to get some new insight on the "structural origin" of shear-banding. These studies essentially confirmed what had been established in the 90s, i.e. that shear-banding in wormlike micelles is correlated with a flow-induced alignment of the Kuhn segments of the worms. Close to an equilibrium isotropic/nematic transition, the flow alignment produces a true nematic order, whereas further away from the transition no structure factor indicative of a nematic order can be observed[3,4]. Such alignment naturally has signatures on the SANS or flow birefringence patterns. The merit of recent structural studies may reside in their impetus to put forth the possible influence of the concentration field on shear-banding transitions. Nevertheless the idea is not new[6] and it is unfortunate to notice that a seminal study like that of Schmitt *et al.*[27] on the role of flow-concentration coupling in shear-induced phase separation of complex fluids has been overlooked by most recent structural studies. Experimentally, concentration effects sometimes called shear-induced demixing have been observed at different scales. On the one hand, it has been known for years (see Lerouge *et al.* for a review[4]) that some shear-banding transitions are associated with the appearance of turbidity, mostly co-localized with the other banded patterns (of birefringence, of viscosity and shear-rate, etc.). Such turbidity must be connected to some types of mesoscopic structures with characteristic sizes ranging in the microns, and flow-concentration coupling has long been invoked to rationalize such fact[4]. Qualitatively, flow-concentration coupling in living polymers is probably connected to the mechanism developed for regular polymers by Helfand and Fredrickson[135]. Unfortunately quantitative data about the resulting micron-size structures are still lagging behind. A recent study focused on regular polymers could lay the ground for further developments in that direction[136]. Note however that concentration effects at large scale are not a necessary ingredient for shear-banding since some shear-banding flows are not associated with visible turbidity[4,23,25,33]. On the other hand, in the recent spatially-resolved SANS experiments focusing on small scale concentration effects, no concentration gradient of surfactant molecules between bands was observed in a semi-dilute sample exhibiting a turbid high shear rate band[13] while such a concentration gradient at small scale was detected in a concentrated sample in the absence of turbidity[25]. These last studies open interesting

perspectives but they are still far from elucidating the mechanisms of shear-banding, first because they are limited to the investigation of two fluids and second because they ignore the potential impact of flow instabilities on the reliability of the structural measurements, leading to conclusions that should be taken with care. Furthermore, the overall picture across the different concentration regimes is far from being sorted out since the correlation between the degree of SIS turbidity and the surfactant and salt concentrations of the sample is clearly not simple. In particular, salt content is known to have an impact on turbidity[33]. In our opinion, the quantification of the relation between salt content and turbidity and its theoretical rationalization should be a priority for researchers involved in a structural approach. Is the unexplained impact of salt content on turbidity in the nonlinear regime connected with the variation of viscosity in the linear regime? Is flow-concentration coupling connected with stress diffusion and the turbidity to the value of ℓ? Is there a link between turbidity and wall slip?

On the hydrodynamical side of the problem, much progress has been made in the past few years. Note that this approach toward flows of living polymers was essentially non-existent a few years ago. Many efforts have been made since then to connect the emergence of complex flows in living polymers to the phenomenology of viscoelastic instabilities originally developed for regular polymers. In contrast to recent structural studies, hydrodynamical studies do acknowledge the other side of the problem; they simply observe that many of the structural properties of the fluid are not directly relevant at the macroscopic scale. The strength of normal stresses seems to be the most important factor in determining the thresholds of instabilities, just like in polymer solutions. From this perspective, studies on living polymers offer a test ground for the universality of viscoelastic instabilities. The influence of shear-banding (or other stratifications) has been studied quite extensively[43]. More recently, the impact of shear-thinning and shear-thickening due to SIS has also been tested[34,35], but more studies in that direction would be welcomed. The potential existence of viscoelastic instabilities in concentrated ordered phases, in particular exhibiting yield stress, remains a tantalizing possibility[36]. In each case, the microstructural origin of the huge normal stresses that develop in the SIS is clearly an open challenge. Furthermore, many of the challenges awaiting the hydrodynamical approach on living polymers are shared by regular polymers. Is there a nonlinear transition to turbulence in rectilinear shear flows[40]? What is the precise interplay of elasticity and inertia when $\mathscr{E} \sim 1$[42]? How can we understand flow instabilities in transient flows such as LAOS? Recent studies by Casanellas *et al.*[137,138] have started to pave the way in that direction, which we shall follow jointly in an upcoming paper[133]. How can we understand the statistics of elastic turbulence[32]? What are the differences between living and standard polymers? Is there a relation with the microscopic coil-stretch transition, as suggested by Steinberg *et al.*[139]? What is the mechanism of instability in flows dominated by extension like the cross-slot flow[140]? What about viscoelastic instabilities in flows with free surfaces? Only a few exploratory studies have touched on this latest question, from the perspective of the Faraday instability[141], of the Rayleigh-Plateau instability[142], and of the dynamics of bubbles[143]. In any case, the most important task is probably to be able to define a relevant Weissenberg (and/or Reynolds, we call it *S*) number. In many cases in living polymers, the time scales involved in the definition are not trivial. Structural and hydrodynamical transitions can influence the time scale of the flow $1/\dot{\gamma}$, and that of the fluid τ. Superposition rheometry offers one possible way to assess such nonlinearity by measuring some variation of fluid time with $\dot{\gamma}$[144,145]. Whether or not such fluid time scale is the one (τ) relevant for the definition of *S* remains unknown.

Acknowledgements: The authors thank Jn. Alonzo Ríos Mira for critical review of the paper.

References

1 J. T. Padding, W. J. Briels, M. R. Stukan and E. S. Boek, Soft Matter, 2009, **5**, 4367–4375.
2 C. Wang, Z. Wang and X. Zhang, Accounts of Chemical Research, 2012, **45**, 608–618.
3 J. Berret, Molecular Gels, Springer Netherlands, 2006, pp. 667–720.
4 S. Lerouge and J.-F. Berret, Advances in Polymer Science, Polymer Characterization, Springer Berlin / Heidelberg, 2010, vol. 230, pp. 1–71.
5 M. E. Cates and S. M. Fielding, Advances in Physics, 2006, **55**, 799–879.
6 S. M. Fielding, Soft Matter, 2007, **3**, 1262–1279.
7 P. Callaghan, Rheologica Acta, 2008, **47**, 243–255.
8 S. Manneville, Rheologica Acta, 2008, **47**, 301–318.
9 P. Olmsted, Rheologica Acta, 2008, **47**, 283–300.
10 J. Dehmoune, J. P. Decruppe, O. Greffier, H. Xu and P. Lindner, Langmuir, 2009, **25**, 7271–7278.
11 M. Takeda, T. Kusano, T. Matsunaga, H. Endo, M. Shibayama and T. Shikata, Langmuir, 2011, **27**, 1731–1738.
12 N. Tepale, E. R. Macias, F. Bautista, J. E. Puig, O. Manero, M. Gradzielski and J. I. Escalante, J. Coll. Inter. Sci., 2011, **363**, 595–600.
13 A. K. Gurnon, C. Lopez-Barron, M. J. Wasbrough, L. Porcar and N. J. Wagner, ACS Macro Letters, 2014, **3**, 276–280.
14 A. Raudsepp and P. T. Callaghan, Soft Matter, 2008, **4**, 784–796.
15 C. R. Lopez-Barron and N. J. Wagner, Soft Matter, 2011, **7**, 10856–10863.
16 P. Thareja, I. H. Hoffmann, M. W. Liberatore, M. E. Helgeson, Y. T. Hu, M. Gradzielski and N. J. Wagner, J. Rheol., 2011, **55**, 1375–1397.

17 J. R. Brown and P. T. Callaghan, Soft Matter, 2011, **7**, 10472–10482.
18 K. G. Wilmsmeyer, X. Zhang and L. A. Madsen, Soft Matter, 2012, **8**, 57–60.
19 A. Raudsepp, P. Callaghan and Y. Hemar, J. Rheol., 2008, **52**, 1113–1129.
20 P. J. Photinos, M. R. Lopez-Gonzalez, C. V. Hoven and P. T. Callaghan, Phys. Rev. E, 2010, **82**, 011502.
21 P. Photinos, Liquid Crystals, 2010, **37**, 695–700.
22 M. E. Helgeson, M. D. Reichert, Y. T. Hu and N. J. Wagner, Soft Matter, 2009, **5**, 3858–3869.
23 M. E. Helgeson, P. A. Vasquez, E. W. Kaler and N. J. Wagner, J. Rheol., 2009, **53**, 727–756.
24 M. W. Liberatore, F. Nettesheim, P. A. Vasquez, M. E. Helgeson, N. J. Wagner, E. W. Kaler, L. P. Cook, L. Porcar and Y. T. Hu, J. Rheol., 2009, **53**, 441–458.
25 M. E. Helgeson, L. Porcar, C. Lopez-Barron and N. J. Wagner, Phys. Rev. Lett., 2010, **105**, 084501.
26 A. P. Eberle and L. Porcar, Current Opinion in Colloid & Interface Science, 2012, **17**, 33–43.
27 V. Schmitt, C. M. Marques and F. Lequeux, Physical Review E, 1995, **52**, 4009.
28 M. A. Fardin, T. Divoux, M. A. Guedeau-Boudeville, I. Buchet-Maulien, J. Browaeys, G. H. McKinley, S. Manneville and S. Lerouge, Soft Matter, 2012, **8**, 2535–2553.
29 S. Lerouge, J.-P. Decruppe and P. Olmsted, Langmuir, 2004, **20**, 11355–11365.
30 S. Lerouge, M. A. Fardin, M. Argentina, G. Gregoire and O. Cardoso, Soft Matter, 2008, **4**, 1808–1819.
31 M. A. Fardin, B. Lasne, O. Cardoso, G. Grégoire, M. Argentina, J. P. Decruppe and S. Lerouge, Phys. Rev. Lett., 2009, **103**, 028302.
32 M. A. Fardin, D. Lopez, J. Croso, G. Grégoire, O. Cardoso, G. H. McKinley and S. Lerouge, Phys. Rev. Lett., 2010, **104**, 178303.
33 M. A. Fardin, T. J. Ober, V. Grenard, T. Divoux, S. Manneville, G. H. McKinley and S. Lerouge, Soft Matter, 2012, **8**, 10072–10089.
34 M. A. Fardin, C. Perge, N. Taberlet and S. Manneville, Phys. Rev. E, 2014, **89**, 011001.
35 C. Perge, M.-A. Fardin and S. Manneville, Soft Matter, 2014, **10**, 1450–1454.
36 C. Perge, M. A. Fardin and M. S., Eur. Phys. J. E, 2014, –.
37 P. Decruppe, J. L. Bécu, O. Greffier and N. Fazel, Phys. Rev. Lett., 2010, **105**, 258301.
38 R. Larson, Rheol. Acta, 1992, **31**, 213–263.
39 R. Larson, E. S. Shaqfeh and S. Muller, J. Fluid Mech, 1990, **218**, 573–600.
40 A. N. Morozov and W. van Saarloos, Phys. Rep., 2007, **447**, 112–143.
41 S. J. Muller, Korea-Aust. Rheol. Journal, 2008, **20**, 117–125.
42 M. Fardin, C. Perge and N. Taberlet, Soft Matter, 2014, **10**, 3523–3535.
43 M.-A. Fardin and S. Lerouge, The Eur. Phys. J. E, 2012, **35**, 1–29.
44 J. K. Dhont and W. J. Briels, Rheologica Acta, 2008, **47**, 257–281.
45 J. K. G. Dhont, K. Kang, M. P. Lettinga and W. J. Briels, Korea-Aust. Rheol. Journal, 2010, **22**, 291–308.
46 J. Dehmoune, J. P. Decruppe, O. Greffier and H. Xu, J. Rheol., 2008, **52**, 923–940.
47 M. Vasudevan, A. Shen, B. Khomami and R. Sureshkumar, J. Rheol., 2008, **52**, 527–550.
48 V. Lutz-Bueno, J. Kohlbrecher and P. Fischer, Rheol. Acta, 2013, **52**, 297–312.
49 V. Herle, S. Manneville and P. Fischer, Eur. Phys. J. E, 2008, **26**, 3–12.
50 J. Dehmoune, S. Manneville and J.-P. Decruppe, Langmuir, 2011, **27**, 1108–1115.
51 K. Gasljevic, K. Hoyer and E. F. Matthys, J. Rheol., 2007, **51**, 645–667.
52 R. K. Rodrigues, M. A. da Silva and E. Sabadini, Langmuir, 2008, **24**, 13875–13879.
53 A. Gyr and J. Buehler, J. of Non-Newt. Fluid Mech., 2010, **165**, 672–675.
54 F. Hadri, A. Besq, S. Guillou and R. Makhloufi, J. of Non-Newt. Fluid Mech., 2011, **166**, 326–331.
55 N. A. Tuan and H. Mizunuma, J. Rheol., 2013, **57**, 1819–1832.
56 N. A. Tuan and H. Mizunuma, J. of Non-Newt. Fluid Mech., 2013, **198**, 71–77.
57 T. Gallot, C. Perge, V. Grenard, M.-A. Fardin, N. Taberlet and S. Manneville, Rev. Sci. Inst., 2013, **84**, 045107.
58 M. A. Fardin, T. J. Ober, C. Gay, G. Grégoire, G. H. McKinley and S. Lerouge, Eur. Phys. Lett., 2011, **96**, 44004.
59 M. Fardin, T. Divoux, M. Guedeau-Boudeville, I. Buchet-Maulien, J. Browaeys, G. McKinley, S. Manneville and S. Lerouge, Soft Matter, 2012, **8**, 2535–2553.
60 J. Beaumont, N. Louvet, T. Divoux, M.-A. Fardin, H. Bodiguel, S. Lerouge, S. Manneville and A. Colin, Soft Matter, 2013, **9**, 735–749.
61 S. Majumdar and A. K. Sood, Phys. Rev. E, 2011, **84**, 015302.
62 R. Ganapathy, S. Majumdar and A. K. Sood, Eur. Phys. J. B, 2008, **64**, 537–542.
63 R. Ganapathy and A. K. Sood, J. of Non-Newt. Fluid Mech., 2008, **149**, 78–86.
64 R. Ganapathy, S. Majumdar and A. K. Sood, Phys. Rev. E, 2008, **78**, 021504.
65 B. Marcos Marin-Santibanez, J. Perez-Gonzalez, L. de Vargas, J. Paul Decruppe and G. Huelsz, J. of Non-Newt. Fluid Mech., 2009, **157**, 117–125.
66 G. R. Moss and J. P. Rothstein, J. of Non-Newt. Fluid Mech., 2010, **165**, 1505–1515.
67 G. R. Moss and J. P. Rothstein, J. of Non-Newt. Fluid Mech., 2010, **165**, 1–13.
68 N. Kumar, S. Majumdar, A. Sood, R. Govindarajan, S. Ramaswamy and A. K. Sood, Soft Matter, 2012, **8**, 4310–4313.
69 T. McLeish, Advances in physics, 2002, **51**, 1379–1527.
70 S. Milner, T. McLeish and A. Likhtman, J. Rheol., 2001, **45**,

539.
71 W. Zou and R. G. Larson, J. Rheol.), 2014, **58**, 681–721.
72 R. L. Moorcroft and S. M. Fielding, Phys. Rev. Lett., 2013, **110**, 086001.
73 K. Sato, X.-F. Yuan and T. Kawakatsu, The Eur. Phys. J. E, 2010, **31**, 135–144.
74 M. A. Fardin, T. J. Ober, C. Gay, G. Gregoire, G. H. McKinley and S. Lerouge, Soft Matter, 2012, **8**, 910–922.
75 P. E. Boukany and S.-Q. Wang, Macromol., 2008, **41**, 1455–1464.
76 T. Yamamoto, K. Sawa and K. Mori, J. Rheol., 2009, **53**, 1347–1362.
77 M. P. Lettinga and S. Manneville, Phys. Rev. Lett., 2009, **103**, 248302.
78 K. W. Feindel and P. T. Callaghan, Rheol. Acta, 2010, **49**, 1003–1013.
79 J. M. Adams, S. M. Fielding and P. D. Olmsted, J. of Non-Newt. Fluid Mech., 2008, **151**, 101–118.
80 S. M. Fielding, Phys. Rev. Lett., 2010, **104**, 198303.
81 A. Nicolas and A. Morozov, Phys. Rev. Lett., 2012, **108**, 088302.
82 R. Keunings, Rheology reviews, 2004, **2004**, 67–98.
83 R. Bird, R. Armstrong and O. Hassager, Dynamics of polymeric liquids. Vol. 2: Kinetic theory., John Wiley and Sons Inc., New York, NY, 1987.
84 F. Bautista, M. Munoz, J. Castillo-Tejas, J. H. Perez-Lopez, J. E. Puig and O. Manero, J. Phys. Chem. B, 2009, **113**, 16101–16109.
85 B. Garcia-Rojas, F. Bautista, J. E. Puig and O. Manero, Phys. Rev. E, 2009, **80**, 036313.
86 J. P. Garcia-Sandoval, O. Manero, F. Bautista and J. E. Puig, J. of Non-Newt. Fluid Mech., 2012, **179**, 43–54.
87 D. Lopez-Diaz, E. Sarmiento-Gomez, C. Garza and R. Castillo, J. Coll. & Inter. Sci., 2010, **348**, 152–158.
88 F. Bautista, V. V. A. Fernandez, E. R. Macias, J. H. Perez-Lopez, J. I. Escalante, J. E. Puig and O. Manero, J. of Non-Newt. Fluid Mech., 2012, **177**, 89–96.
89 H. T. Jahromi, M. Webster, J. Aguayo and O. Manero, Journal of Non-Newtonian Fluid Mechanics, 2011, **166**, 102 – 117.
90 L. Zhou, P. A. Vasquez, L. P. Cook and G. H. McKinley, J. Rheol., 2008, **52**, 591–623.
91 C. J. Pipe, N. J. Kim, P. A. Vasquez, L. P. Cook and G. H. McKinley, J. Rheol.), 2010, **54**, 881–913.
92 L. Zhou, L. P. Cook and G. H. McKinley, Siam J. Appl. Math., 2012, **72**, 1192–1212.
93 N. Germann, L. P. Cook and A. N. Beris, J. of Non-Newt. Fluid Mech., 2013, **196**, 51–57.
94 M. Cromer, L. P. Cook and G. H. McKinley, J. of Non-Newt. Fluid Mech., 2011, **166**, 566–577.
95 P. A. Vasquez, G. H. McKinley and L. P. Cook, J. Non-Newt. Fluid Mech., 2007, **144**, 122–139.
96 P. Nghe, S. M. Fielding, P. Tabeling and A. Ajdari, Phys. Rev. Lett., 2010, **104**, 248303.
97 S. J. Haward and G. H. McKinley, Phys. Rev. E, 2012, **85**, 031502.
98 M. Vasudevan, E. Buse, D. Lu, H. Krishna, R. Kalyanaraman, A. Q. Shen, B. Khomami and R. Sureshkumar, Nature Mat., 2010, **9**, 436–441.
99 C. J. Pipe, T. S. Majmudar and G. H. McKinley, Rheol. Acta, 2008, **47**, 621–642.
100 P. Nghe, G. Degré, P. Tabeling and A. Ajdari, Applied Physics Letters, 2008, **93**, 204102.
101 S. M. Fielding and H. J. Wilson, J. of Non-Newt. Fluid Mech., 2010, **165**, 196–202.
102 M. Cromer, L. P. Cook and G. H. McKinley, J. of Non-Newt. Fluid Mech., 2011, **166**, 180–193.
103 C. Masselon, J.-B. Salmon and A. Colin, Phys. Rev. Lett., 2008, **100**, 038301.
104 C. Masselon, A. Colin and P. D. Olmsted, Phys. Rev. E, 2010, **81**, 021502.
105 J. P. Rothstein, Rheology reviews. The British Society of Rheology, 2008, 1–46.
106 A. Bhardwaj, D. Richter, M. Chellamuthu and J. Rothstein, Rheologica Acta, 2007, **46**, 861–875.
107 M. Chellamuthu and J. R. Rothstein, J. Rheol., 2008, **52**, 865–884.
108 E. Miller, C. Clasen and J. P. Rothstein, Rheol. Acta, 2009, **48**, 625–639.
109 T. Takahashi and D. Sakata, J. Rheol., 2011, **55**, 225–240.
110 N. J. Kim, C. J. Pipe, K. H. Ahn, S. J. Lee and G. H. McKinley, Korea-Aust. Rheol. Journal, 2010, **22**, 31–41.
111 T. Perkins, D. Smith and S. Chu, Science, 1997, **276**, 2016.
112 P. Stone, S. Hudson, P. Dalhaimer, D. Discher, E. Amis and K. Migler, Macromol., 2006, **39**, 7144–7148.
113 T. J. Ober, J. Soulages and G. H. McKinley, J. Rheol., 2011, **55**, 1127–1159.
114 T. J. Ober, S. J. Haward, C. J. Pipe, J. Soulages and G. H. McKinley, Rheol. Acta, 2013, **52**, 529–546.
115 S. J. Haward, T. J. Ober, M. S. N. Oliveira, M. A. Alves and G. H. McKinley, Soft Matter, 2012, **8**, 536–555.
116 N. Dubash, P. Cheung and A. Q. Shen, Soft Matter, 2012, **8**, 5847–5856.
117 J. Pathak and S. Hudson, Macromol., 2006, **39**, 8782–8792.
118 P. Arratia, C. Thomas, J. Diorio and J. Gollub, Phys. Rev. Lett., 2006, **96**, 144502.
119 R. Poole, M. Alves and P. Oliveira, Phys. Rev. Lett., 2007, **99**, 164503.
120 S. Haward, F. Galindo-Rosales, P. Ballesta and M. Alves, Applied Physics Letters, 2014, **104**, 124101.
121 M. Pasquali, Nat Mater, 2010, **9**, 381–382.
122 N. Dubash, J. Cardiel, P. Cheung and A. Q. Shen, Soft Matter, 2011, **7**, 876–879.
123 P. Cheung, N. Dubash and A. Q. Shen, Soft Matter, 2012, **8**, 2304–2309.
124 J. J. Cardiel, L. Tonggu, A. C. Dohnalkova, P. de la Iglesia, D. C. Pozzo, L. Wang and A. Q. Shen, ACS Nano, 2013, **7**, 9704–9713.
125 J. J. Cardiel, L. Tonggu, P. de la Iglesia, Y. Zhao, D. C. Pozzo,

L. Wang and A. Q. Shen, Langmuir, 2013, **29**, 15485–15495.
126 J. J. Cardiel, A. C. Dohnalkova, N. Dubash, Y. Zhao, P. Cheung and A. Q. Shen, PNAS, 2013, **110**, E1653–E1660.
127 R. H. Ewoldt, A. E. Hosoi and G. H. McKinley, J. Rheol., 2008, **52**, 1427–1458.
128 C. J. Dimitriou, L. Casanellas, T. J. Ober and G. H. McKinley, Rheol. Acta, 2012, **51**, 395–411.
129 S. Rogers, J. Kohlbrecher and M. P. Lettinga, Soft Matter, 2012, **8**, 7831–7839.
130 A. K. Gurnon, C. R. Lopez-Barron, A. P. R. Eberle, L. Porcar and N. J. Wagner, Soft Matter, 2014, **10**, 2889–2898.
131 L. Zhou, L. P. Cook and G. H. McKinley, J. of Non-Newt. Fluid Mech., 2010, **165**, 1462–1472.
132 A. K. Gurnon and N. J. Wagner, J. Rheol., 2012, **56**, 333–351.
133 M. Fardin, C. Perge, L. Casanellas, T. Hollis, N. Taberlet, J. Ortín, S. Lerouge and S. Manneville, Rheol. Acta, 2014, under review.
134 N. S. M. Yusof and M. Ashokkumar, Soft Matter, 2013, **9**, 1997–2002.
135 E. Helfand and G. H. Fredrickson, Phys. Rev. Lett., 1989, **62**, 2468.
136 M. Cromer, M. C. Villet, G. H. Fredrickson and L. G. Leal, Phys. of Fluids, 2013, **25**, 051703.
137 L. Casanellas and J. Ortin, Rheol. Acta, 2012, **51**, 545–557.
138 L. Casanellas and J. Ortin, J. Rheol., 2014, **58**, 149–181.
139 S. Gerashchenko, C. Chevallard and V. Steinberg, Eur. Phys. Lett., 2005, **71**, 221.
140 S. Haward and G. McKinley, Physics of Fluids, 2013, **25**, 083104.
141 T. Epstein and R. D. Deegan, Phys. Rev. E, 2010, **81**, 066310–066310.
142 F. Boulogne, M. A. Fardin, S. Lerouge, L. Pauchard and F. Giorgiutti-Dauphine, Soft Matter, 2013, **9**, 7787–7796.
143 V. Vidal, F. Soubiran, T. Divoux and J.-C. Géminard, Phys. Rev. E, 2011, **84**, 066302.
144 P. Ballesta, M. P. Lettinga and S. Manneville, J. Rheol., 2007, **51**, 1047–1072.
145 S. Kim, J. Mewis, C. Clasen and J. Vermant, Rheol. Acta, 2013, **52**, 727–740.

We highlight recent progress on flows of living polymer fluids, from their microscopic structure to their macroscopic hydrodynamics.

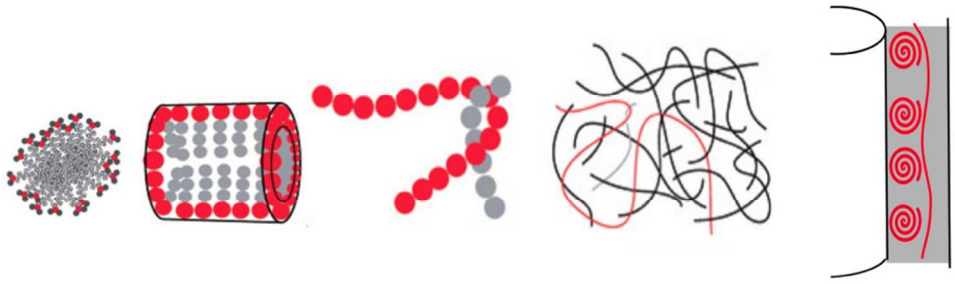

We highlight recent progress on flows of living polymer fluids, from their microscopic structure to their macroscopic hydrodynamics.
354x111mm (72 x 72 DPI)